In situ tuning the optical properties of a cavity by wrinkling

Branko Kolaric,[1,a)] Hugues Vandeparre,[1] Sylvain Desprez,[2] Renaud A. L. Vallée,[3] and Pascal Damman[1]

[1]*Laboratoire Interfaces and Fluides Complexes, Centre d' Innovation et de Recherche en Matériaux Polymères, Université de Mons, 20 Place du Parc, B-7000 Mons, Belgium*
[2]*Materia Nova, Avenue Nicolas Copernic 1, B-7000 Mons, Belgium*
[3]*Centre de Recherche Paul Pascal (CNRS-UPR8641), 115 avenue du docteur Schweitzer, 33600 Pessac, France*

(Received 16 October 2009; accepted 21 December 2009; published online 28 January 2010)

In this letter we propose an original, *in situ*, approach to tune the optical properties of an optical cavity, based on the wrinkling of compressed metal/polymer multilayer thin films. This phenomenon is conceptually described, simulated, and experimentally confirmed. The main idea is to use wrinkling to modulate the effective refractive index of the upper interface. This modulation induces a spectral shift of the cavity modes. The work presented here constitutes a first step to the development of stretchable and curved photonics. © *2010 American Institute of Physics*. [doi:10.1063/1.3298740]

Optical cavities, like a Fabry–Pérot resonator, can be easily designed by inserting a dielectric slab between two parallel, highly reflecting surfaces. Up to date, numerous structures have been described in the literature,[1,2] with applications ranging from atomic physics[3,4] to biosensing, optoelectronics, and chemistry.[1,5] Beyond the classical spectral selection of an electromagnetic field mode, it was recently suggested to use optical cavities to harness quantum effects in quantum cryptography and quantum computing.[1,2,4–6] One step further, designing microcavities with switchable optical properties (frequency, intensity, and/or finesse) by act of an external stimulus (mechanical, thermal, electrical, or chemical) remains a challenging task.

Recently, wrinkling of compressed multilayer thin films has attracted much interest because of its simple, cost-effective, and well-defined way to generate nanomicrotopographies on large areas. The creation of a diversity of wavy structures ranging from the classical striped and labyrinthine patterns to the more sophisticated herringbone and splaying fanlike geometries[7–11] can be performed by varying the applied stress field. This considerable flexibility has allowed researchers to design microlens arrays,[12] nanofluidic devices,[13] surface relief diffusers,[14] stretchable electronics,[15] and tunable electro-optical devices.[16,20,21] Furthermore, it offered a convenient way to study some physical properties, like wetting[10] and adhesion[17] of surfaces or cells.[18] Finally, researchers used wrinkling to determine some characteristic parameters of thin films, thickness and elastic properties.[19]

In this Letter, we develop a strategy, based on this self-organized process, to tune the optical properties of microcavities.

The used optical cavities are made of a thin titanium (Ti) layer and a thick silicon (SiO_x) wafer. These two reflecting surfaces are separated by a thin polystyrene (PS) film [Fig. 1(c)]. Two steps were necessary to build up this hybrid multilayer microcavity as follows: (i) Spin-coating of high molecular weight atactic PS solutions in toluene (MW $\simeq 1450$ kDa) on bare silicon substrates to produce films with thicknesses of about 1 μm and (ii) Deposition of thin Ti layers with thicknesses ranging from 10 to 20 nm onto the polymer by thermal evaporation. Wrinkling is induced by heating the whole system at 200 °C, i.e., 95 °C above the glass transition temperature T_g of PS. The mismatch in thermal expansion coefficients between the Ti membrane and the silicon substrate induces a compressive stress in the metal layer during the heating process. Once above T_g, the softening of PS induces a relaxation of this stress and wrinkling takes place.[8] The thermal treatment being isotropic, labyrinthine patterns form to relax the stress equally in all directions. The resulting metal surfaces were examined by optical microscopy. The optical properties of the cavity were investigated by reflection spectroscopy (UV-Vis-NIR Varian Cary 5G spectrophotometer).

Additionally, we performed simulations using the finite-difference time-domain method,[22] integrated in a freely available software package with subpixel smoothing for increased accuracy.[23] In order to be in close agreement with the experimental conditions, the multilayer films were designed as followed: (i) a first sample with a PS (dielectric constant of 2.53) slab of 1.42 μm thickness was set on a substrate with a dielectric constant of 11.9 (silicon) extending to the Perfectly Matched Layers (PMLs) in the z-direction; (ii) a second sample was created, starting from this first sample and adding a second 20 nm thick slab of titania (dielectric constant of 3.61) on top of the PS slab; (iii) finally, the wrinkled sample was designed from the first sample by digging from the top of the PS slab, in a triangular type of wave pattern, five titania steps, 20 nm thick and 0.1 μm wide, down followed by five steps up, thus accounting for the 100 nm depth and 1 μm periodicity of the wrinkles experimentally measured.

Due to the constructive and destructive interferences of the optical waves inside the cavity, some modes can settle, as shown in the reflection spectra of Fig. 1(a). The PS slab [Fig. 1(a)] is sufficient by itself to create a weak cavity effect. In order to enhance the strength of the cavity, we covered the PS slab with a few nanometer thick highly reflecting Ti membrane [Fig. 1(c)]. The presence of titanium on top of the film, which has a much higher refractive index than air, in-

a)Electronic mail: branko.kolaric@umons.ac.be.

Author complimentary copy. Redistribution subject to AIP license or copyright, see http://apl.aip.org/apl/copyright.jsp

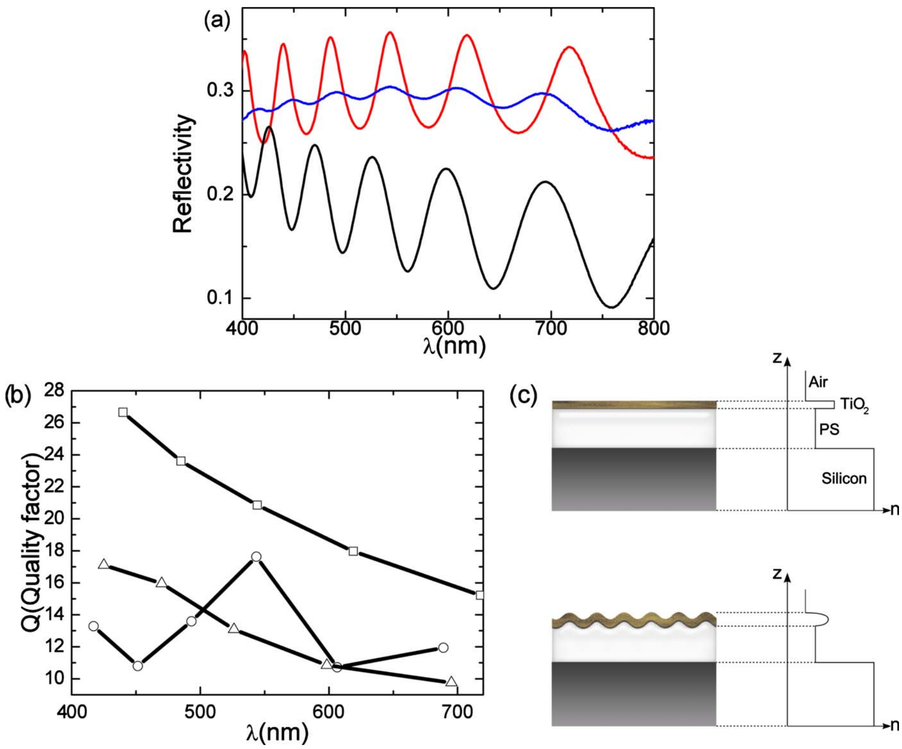

FIG. 1. (Color online) Experimental Schematic structures (c) and corresponding reflection spectra (a) of the various cavities studied in this letter (black: PS layer, red: PS layer with Ti deposit on the top, blue: PS with wrinkled Ti layer); (b) calculated Q factor for various cavities, PS △, PS with Ti deposit on the top □, PS with wrinkled Ti layer ○, and (c) scheme of the various cavities studied in this letter.

creases the cavity effect and causes a redshift of the cavity modes [Fig. 1(a)]. Interestingly, wrinkled systems exhibit a blueshift of the resonance peaks in the reflection spectrum [Fig. 1(a)] due to the decrease in the effective refractive index of the top interface [Fig. 1(c)], the latter being a combination of the refractive indexes of polymer, air, and titanium, in an effective medium approach. These results clearly show that we can control the effective refractive index of the upper surface by controlling the wrinkles morphology. In contrast to what is expected, the growth of wrinkles does not simply suppress the optical cavity effect but allows a modulation of the optical properties of the multilayer. However, an increase in the top surface roughness caused by wrinkling induces more light scattering and causes the resonance peak to drop in intensity, thereby reducing its quality factor Q [Fig. 1(b)]. We quantify the quality of the cavity by measuring its quality factor Q [Fig. 1(b)], as a function of wavelength, defined as the ratio of the resonant frequency by the bandwidth of the resonance (FWHM of the considered peak). $1/Q$ is thus the fractional bandwidth of the resonance and the lowest is its value, the sharpest is the resonance peak and the strongest is the cavity effect obtained. Figures 1(a) and 1(b) clearly show the resulting narrowing of the peaks and thus the increased quality factor of the Ti covered cavity.

Simulation results are presented in Fig. 2, which shows the cuts in the *xz*-plane of the refractive index (a) and electric field amplitude (b) profiles for the modes corresponding to the peaks situated between 560–580 nm in the simulated reflection spectra (c) of the various structures. The results presented in Figs. 2(a) and 2(b) clearly exhibit a strong correlation between the refractive index profile and the longitudinal electric field mode profile: the y-polarized component of the *z*-incoming (from the top of the structure) electric field profile bends around the high refractive index zone consti-

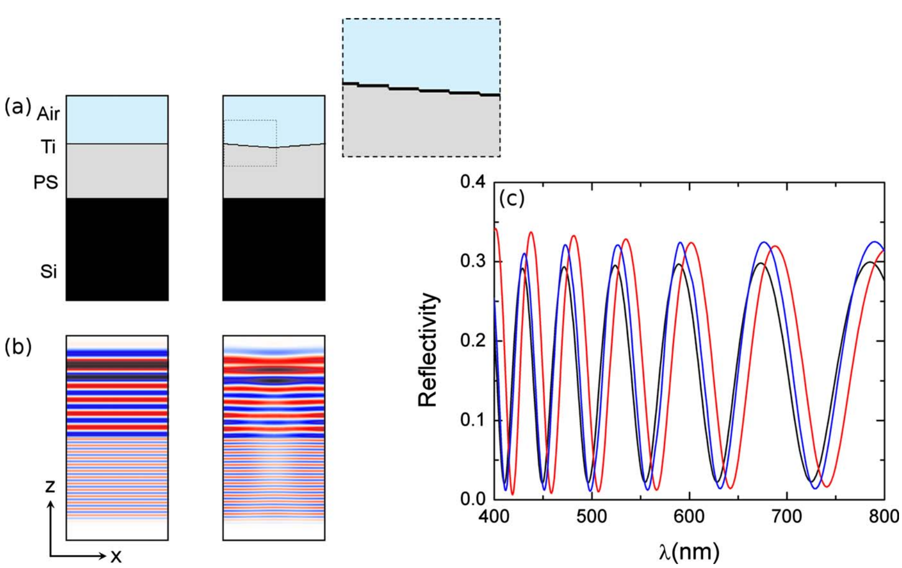

FIG. 2. (Color online) *Simulations* Refractive index profile (a) and corresponding longitudinal electric field mode profile (b) in the cases of non-wrinkled and wrinkled cavities for the 550 nm resonance peak shown in (c). (c) Simulated reflection spectra of the various cavities investigated in this study, the color notation is the same as in Fig. 1(a).

Author complimentary copy. Redistribution subject to AIP license or copyright, see http://apl.aip.org/apl/copyright.jsp

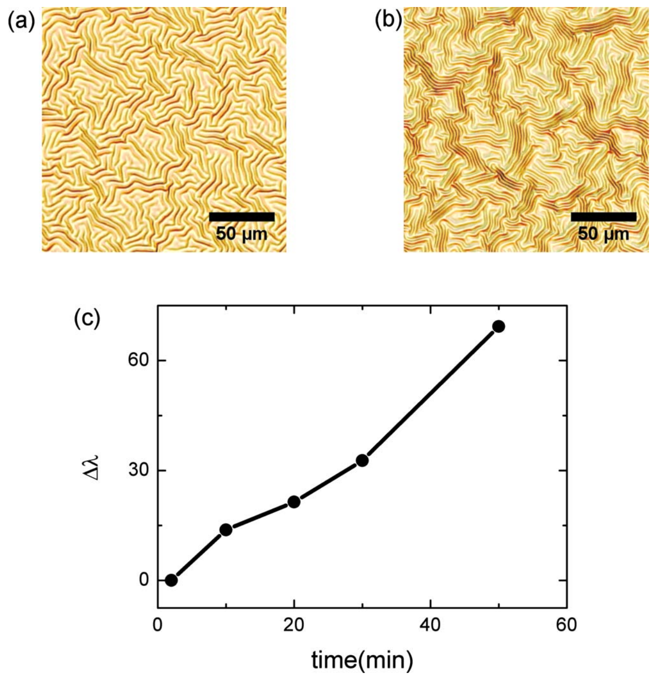

FIG. 3. (Color online) *Influence of roughness on the cavity properties:* Optical micrographs of $Ti/PS/SiO_x$ wrinkled surfaces obtained for a 15 nm thick metal layer deposited on top of a 1, 5 μm PS slab annealed at 200 °C for 2 min (a) and 50 min (b) (scale bar 30 μm). (c) The shift of the reflection maxima at 667 nm for samples annealed for 2, 10, 20, 30, and 50 min.

tuted by the TiO_2 wrinkling, featuring the fact that a mode tends to concentrate its displacement energy in regions of high dielectric constant, while remaining orthogonal to the modes below it in frequency.[24] The bending of the electric field induced by wrinkling might be responsible for the observed enhancement (effect of curvature) of the experimentally determined quality factor at 550 nm in Fig. 1(b). Associated to this wrinkling-induced mode profile change, one can also see the appearance of white trails (losses) in the bottom part of the structure Fig. 2(b), explaining the intensity drop in the simulated spectrum of the wrinkled structure as compared to the flat TiO_2 layer. However, the attenuation observed in simulations is not comparable to the experimentally measured one due to the fact that the degree of roughness intrinsically obtained in the wrinkling experiment has not been addressed in the simulations.

To investigate the effect of roughness on the cavity properties of our system, we annealed various identical samples at 200 °C for increasing times. As shown in Figs. 3(a) and 3(b), we observe a change in the wrinkle morphology. At very short annealing times, a continuous wavy labyrinthine pattern is obtained. Increasing the annealing time causes the transition from this labyrinthine pattern to a more discrete island structure.

In fact, the wrinkled pattern induced in the rigid membrane should follow two competing *rules*: (i) the formation of parallel wrinkles with a well-defined wavelength to minimize the energy of the membrane, and (ii) the growth of isotropic patterns (thermal stresses are isotropic). Due to these two effects, the initial patterns are out-of-equilibrium with irregular morphology (Fig. 3). Annealing can be used, however, to drive samples toward the equilibrium morphology, characterized by island of parallel wrinkles domains surrounded by a disordered or flat surface. Interestingly, this coarsening process happens with an accompanying increase in amplitude and roughness. As a result, it is also possible to explore annealing to tune the optical properties of our cavities. Increasing annealing time causes a decrease in the effective refractive index of the top interface and thus a more pronounced blueshift of the resonance peaks. The tuning is visible in [Fig. 3(c)] as a shift of the reflection maximum (at 667 nm) measured as a function of annealing time. As a caveat however, we have to point out that an increase in roughness raises the scattering so that the cavity effect finally vanishes for very long annealing times. In summary, we have developed a strategy able to allow us to tune the cavity properties of hybrid multilayer thin films based on the wrinkling mechanism. Interestingly, the proposed approach is nondestructive and is used *in situ*. Our results clearly show that controlling the morphology of the wrinkles could lead to the fabrication of large-scale nanosensor devices.

The authors warmly acknowledge the assistance of Thomas Godfroid and Fabian Renaux (Materia Nova-MONS) during the reflection experiments. This work was supported by the FRS-FNRS. S.D. and B.K. acknowledge financial support from Region Wallone and EU for a Smart film grant 830039 (ECV12020020892F) in the framework of Convergence project.

[1]M. Trupke, E. A. Hinds, and S. Eriksson, Appl. Phys. Lett. **87**, 211106 (2005).
[2]S. M. Dutra, *Cavity Quantum Electrodynamics: The Strange Theory of Light in a Box* (Wiley, Hoboken, New Jersey, 2005).
[3]H. P. Specht, J. Bochmann, M. Muecke, B. Weber, E. Figueroa, D. L. Moehring, and G. Rempe, Nat. Photonics **3**, 469 (2009).
[4]R. N. Nogueira, A. L. Teixeira, P. S. Andre, J. F. de Rocha, and J. L. Pinto, Opt. Commun. **259**, 110 (2006).
[5]M. L. Terraciano, R. Olson Knell, D. G. Norris, J. Jing, A. Fernández, and L. A. Orozco, Nat. Phys. **5**, 480 (2009).
[6]M. Paternostro, G. S. Agarwal, and M. S. Kim, New J. Phys. **11**, 013059 (2009).
[7]N. Bowden, S. Britain, A. G. Evans, J. W. Hutchinson, and G. M. Whitesides, Nature (London) **393**, 146 (1998).
[8]H. Vandeparre, J. Leopoldes, C. Poulard, S. Desprez, G. Derue, C. Gay, and P. Damman, Phys. Rev. Lett. **99**, 188302 (2007).
[9]H. Vandeparre and P. Damman, Phys. Rev. Lett. **101**, 124301 (2008).
[10]P.-C. Lin and S. Yang, Appl. Phys. Lett. **90**, 241903 (2007).
[11]S. J. Kwon, P. J. Yoo, and H. H. Lee, Appl. Phys. Lett. **84**, 4487 (2004).
[12]E. P. Chan and A. J. Crosby, Adv. Mater. **18**, 3238 (2006).
[13]Y. Mei, D. J. Thurmer, F. Cavallo, S. Kiravittaya, and O. G. Schmidt, Adv. Mater. **19**, 2124 (2007).
[14]J. H. Wang, C. F. Chen, J. R. Ho, T. K. Shih, C. C. Chen, W. T. Whang, and J. Y. Yang, Opt. Laser Technol. **41**, 804 (2009).
[15]D.-Y. Khang, H. Jiang, Y. Huang, and J. A. Rogers, Science **311**, 208 (2006).
[16]C. V. Brown, G. G. Wells, M. I. Newton, and G. McHale, Nat. Photonics **3**, 403 (2009).
[17]E. P. Chan, E. J. Smith, R. C. Hayward, and A. J. Crosby, Adv. Mater. **20**, 711 (2008).
[18]H. Vandeparre, S. Gabriele, S. Desbief, R. Lazzaroni, C. Gay, and P. Damman (unpublished).
[19]J. Huang, M. Juszkiewicz, W. H. de Jeu, E. Cerda, T. Emrick, N. Menon, and T. P. Russell, Science **317**, 650 (2007).
[20]J. Bravo-Abad, A. Rodriguez, P. Bermel, S. G. Johnson, J. D. Joannopoulos, and M. Soljacic, Opt. Express **15**, 16161 (2007).
[21]V. V. Tsukruk, H. Ko, and S. Peleshanko, Phys. Rev. Lett. **92**, 065502 (2004).
[22]A. Taflove and S. C. Hagness, *Computational Electrodynamics: The Finite-Difference Time-Domain Method*, 3rd ed. (Artech House, Norwood, MA, 2005).
[23]A. Farjadpour, D. Roundy, A. Rodriguez, M. Ibanescu, P. Bermel, J. D. Joannopoulos, G. S. Johnson, and G. W. Burr, Opt. Lett. **31**, 2972 (2006).
[24]J. D. Joannopoulos, R. D. Meade, and J. N. Winn, *Photonic Crystals: Molding the Flow of Light* (Princeton University Press, Princeton, New Jersey, 1995), Chap. 2, 16.

Author complimentary copy. Redistribution subject to AIP license or copyright, see http://apl.aip.org/apl/copyright.jsp